Magnetic order in the pseudogap phase of $HgBa_2CuO_{4+\delta}$ studied by spin-polarized neutron diffraction

Yuan Li,[1,*] V. Balédent,[2] N. Barišić,[3,4] Y. C. Cho,[5] Y. Sidis,[2] G. Yu,[6] X. Zhao,[3,7] P. Bourges,[2] and M. Greven[6,†]

[1]*Department of Physics, Stanford University, Stanford, California 94305, USA*

[2]*Laboratoire Léon Brillouin, CEA-CNRS, CEA-Saclay, F-91191 Gif sur Yvette, France*

[3]*T.H. Geballe Laboratory for Advanced Materials, Stanford University, Stanford, California 94305, USA*

[4]*1. Physikalisches Institut, Universität Stuttgart, D-70550 Stuttgart, Germany*

[5]*BK21 Team and Department of Nano Fusion Technology, Pusan National University, Miryang 627-706, Republic of Korea*

[6]*School of Physics and Astronomy, University of Minnesota, Minneapolis, Minnesota 55455, USA*

[7]*State Key Lab of Inorganic Synthesis and Preparative Chemistry, College of Chemistry, Jilin University, Changchun 130012, China*

(Received 19 September 2011; revised manuscript received 7 November 2011; published 16 December 2011)

Spin-polarized neutron diffraction experiments have revealed an unusual $q = 0$ magnetic order in the model high-temperature superconductor $HgBa_2CuO_{4+\delta}$ (Hg1201) below the pseudogap temperature T^* [Y. Li *et al.*, Nature (London) **455**, 372 (2008)]. Together with results for the structurally more complex compound $YBa_2Cu_3O_{6+\delta}$ (YBCO) [B. Fauqué *et al.*, Phys. Rev. Lett. **96**, 197001 (2006); H.A. Mook *et al.*, Phys. Rev. B **78**, 020506 (2008)], this establishes the universal existence of a genuine novel magnetic phase in underdoped cuprates with high maximal T_c (above 90 K at optimal doping). Here we report a systematic study of an underdoped Hg1201 sample ($T_c = 75$ K), the result of which is consistent with the previously established doping dependence of the magnetic signal. We present an assumption-free analysis of all the data available for Hg1201. Depending on how the hole concentration is estimated, comparison with the results for YBCO leads to different scenarios for the competition between the $q = 0$ magnetic order and the spin-density-wave order found in heavily underdoped YBCO.

DOI: 10.1103/PhysRevB.84.224508 PACS number(s): 74.72.Gh, 75.25.Dk, 61.05.fm

I. INTRODUCTION

The origin of the pseudogap phenomenon in the high-critical-temperature (high-T_c) cuprate superconductors is the subject of ongoing debate.[1] Recent experiments have provided clear evidence for signatures of the pseudogap that are distinctly different from those of superconductivity.[2–14] In particular, time-reversal symmetry is broken below the pseudogap temperature T^* in at least four hole-doped cuprate families.[2–10] Meanwhile, there is increasing evidence that preformed Cooper pairs[15,16] exist only in a relatively limited temperature range above T_c,[11,17–23] well below T^*, and are therefore unlikely to be responsible for the pseudogap phenomenon. These experimental facts strongly suggest that the pseudogap regime of the phase diagram is a genuine new phase of matter in close proximity to superconductivity. It has been proposed that, with increasing doping, the pseudogap phase ends at a quantum critical point underneath the superconducting dome. In this view of the phase diagram, the critical fluctuations of the corresponding order parameter give rise to the "strange metal" behavior at high temperatures and they mediate Cooper pairing.[24]

It has proved a difficult task to identify the order parameter of the pseudogap phase. Among observations in underdoped systems (hole concentration $p < 0.16$), several cuprates are known to exhibit spin-density-wave (SDW) or coupled charge/magnetic "stripe" order: In the underdoped part of the phase diagram, near the doping level $p = x \approx 1/8$, $La_{2-x}Sr_xCuO_4$ (LSCO), and especially $La_{2-x}Ba_xCuO_4$ and $(La,Nd)_{2-x}Sr_xCuO_4$ exhibit an instability toward static stripe order, and T_c is strongly suppressed.[25–27] At lower doping ($p < 0.09$), $YBa_2Cu_3O_{6+x}$ (YBCO) exhibits incommensurate SDW order,[28] but neither the hole doping range of the coexistence between the SDW (or stripe) order and the superconductivity nor the wave vector q is universal between YBCO and LSCO.[29] At higher doping, a different type of long-range magnetic order was discovered by spin-polarized neutron diffraction in YBCO[3] and subsequently in Hg1201.[5] This magnetism is characterized by the ordering wave vector $q = 0$, i.e., it preserves the translational symmetry of the crystal lattice. More recently, evidence for this magnetism was also found in the "low-T_c" compound LSCO (maximum $T_c \sim 40$ K, compared to ~ 93 K in YBCO and ~ 97 K in Hg1201), but in this case the order is of very short range, probably due to a competition with the stripe order[8] or as a result of the higher degree of disorder.[30]

Since it has been observed in structurally rather different compounds, it thus appears that the $q = 0$ magnetism is a generic part of the cuprate phase diagram below optimal doping. Moreover, the order appears to be more robust in compounds with higher T_c, which suggests the intriguing possibility that it plays an important role in the mechanism of superconductivity. Owing to the absence of uniform magnetization, order at $q = 0$ requires multiple magnetic moments with perfect cancellation inside the unit cell. A possible scenario for this to occur in structurally simple tetragonal compounds (such as Hg1201) was first proposed by Varma in his loop-current model.[24,31,32] This theory was motivated by the observation that the energy levels of the planar oxygen $2p$ orbitals in the cuprates are very close to the Fermi level when compared to other $3d$-transition-metal perovskites, and it predicts closed loops of intra-unit-cell quantum electrical currents that flow along the Cu-O and O-O bonds. The pattern with two counter-circulating current loops

per unit cell, producing orbital magnetic moments, is in general agreement with the spin-polarized neutron diffraction results.

In this paper, we present our latest results for the $q = 0$ magnetic order in Hg1201. We also carry out an assumption-free analysis of all the polarized neutron diffraction data that have been obtained so far at five doping levels of Hg1201. After a brief description of the experimental methods in Sec. II, we present our new results and data analysis in Sec. III. In Sec. IV, these results are discussed and compared with findings for YBCO.

II. EXPERIMENTAL METHODS

The spin-polarized neutron diffraction experiments were performed on the cold triple-axis spectrometer 4F1 at the Laboratoire Léon Brillouin in Saclay, France. The experimental setup was similar to that in previous studies.[3–5,8,9] The incident neutron beam was monochromated ($E_i = 13.7$ meV) by the (002) reflection of a double-focusing pyrolytic graphite monochromator, and then spin polarized by a supermirror (bender). The scattered neutrons were analyzed by the (111) reflection of Heusler alloy, which simultaneously selects the final neutron energy (for diffraction, $E_f = E_i$) and spin polarization. The orientation of the neutron spin polarization **P** in the scattering process was controlled by a small guide field (∼10 G), which adiabatically rotates the spin polarization from vertical after the bender to the desired orientation at the sample position, and then back to vertical before the analyzer. This guide field was maintained by permanent magnets placed along the beam path and by Helmholtz coils surrounding the sample position. A Mezei spin flipper was placed between the bender and the sample in order to be able to choose between the spin-flip (SF) and non-spin-flip (NSF) scattering geometries. In our experimental setup, the bender selects the neutron spin state $|+\rangle$ (spin up in the vertical direction), whereas the Heusler analyzer selects neutron spin state $|-\rangle$ (spin down), such that the measured intensity corresponds to SF scattering when there is no electrical current in the Mezei flipper. This results in maximal stability in the SF geometry. Very high flipping ratios (defined as the intensity ratio $R = I_{NSF}/I_{SF}$) of nearly 100 were achieved, which proved to be crucial for the detection of small magnetic signals coincident with nuclear Bragg reflections, which are typically orders of magnitude stronger.

Sizeable Hg1201 crystals were grown by a self-flux method[33] and subsequently heat treated[34] in order to reach the desired homogeneous hole concentration. Such crystals are of rather high quality, as indicated by magnetic susceptibility measurements[24] and the ability to observe the vortex lattice via small-angle neutron scattering.[35] Four underdoped Hg1201 crystals had been studied in our previous work.[5] The new data reported here were obtained on a fifth underdoped crystal with $T_c = 75 \pm 2$ K and an array of about 40 nearly optimally doped crystals ($T_c = 95 \pm 2$ K, same as in Ref. 36). The mass and mosaicity (full width at half maximum measured on strong nuclear Bragg reflections) of the two samples were approximately 0.6 g and 0.5°, and 1.8 g and 2.0°, respectively. The samples were measured with scattering wave vectors $(H\,0\,L)$ in the horizontal scattering plane, where the scattering wave vectors are quoted as $\mathbf{Q} = H\mathbf{a}^* + K\mathbf{b}* + L\mathbf{c}^* \equiv (H\ K\ L)$ in units of the reciprocal lattice vectors, with typical room-temperature values $a^* = b^* = 1.614$ Å^{-1} and $c^* = 0.657$ Å^{-1}. A rigid sample holder was used for the underdoped sample, and all measurements were performed with minimal instrument movement in order to maximize the stability of the experimental conditions. The sample holder for the optimally doped sample was less rigid due to the sample's extensive size. Unlike in Refs. 4 and 8, the small size of our underdoped sample rendered the measurements sensitive to (small) spatial variation of the guide field and to the quality of the bender and of the Heusler analyzer, and prevented us from performing full momentum scans on the magnetic signal.

All our measurements were performed at temperatures above T_c, because in the superconducting state the guide field changes abruptly near the surface of the sample, which leads to a depolarization of the neutron beam. This experimental limitation therefore does not allow us to observe the possible interplay between the superconductivity and the $q = 0$ order.

III. RESULTS

In Figs. 1(a)–1(c), we present spin-polarized neutron diffraction data for the $T_c = 75$ K sample, measured at the (1 0 1) Bragg reflection in three spin-polarization geometries (**P** ∥ **Q**: polarization parallel to the momentum transfer; **P** ⊥ **Q**: polarization in the horizontal scattering plane and perpendicular to the momentum transfer; **P** ∥ **Z**: polarization vertical). The NSF data have been divided by the flipping ratio measured

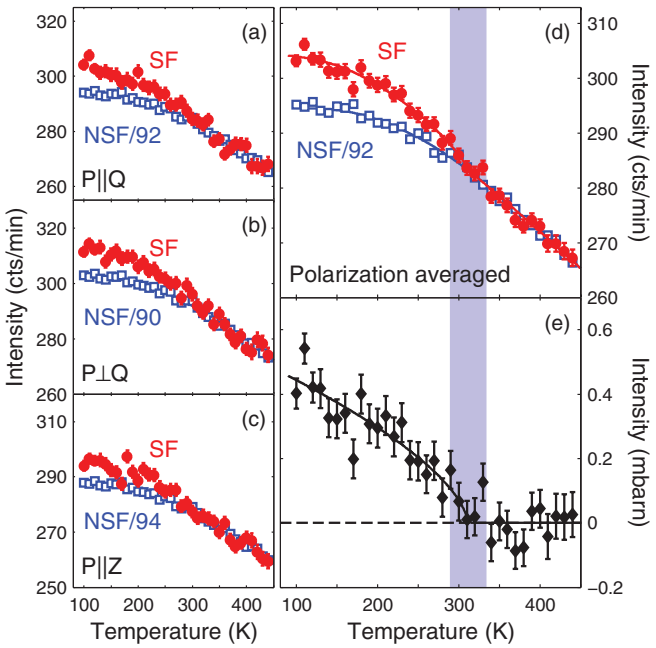

FIG. 1. (Color online) (a)–(c) Temperature dependence of SF and NSF intensities measured at the (1 0 1) Bragg reflection. The NSF intensities are divided by the flipping ratios measured at temperatures above 350 K, where no magnetic signal is expected. (d) The average of all three spin-polarization geometries shows an onset of additional SF intensity below $T_{mag} \approx 320$ K. (e) The deviation of the averaged SF intensity from the (rescaled) NSF intensity is converted into absolute units based on the calculated (1 0 1) nuclear scattering crosssection of 1.26 barn.

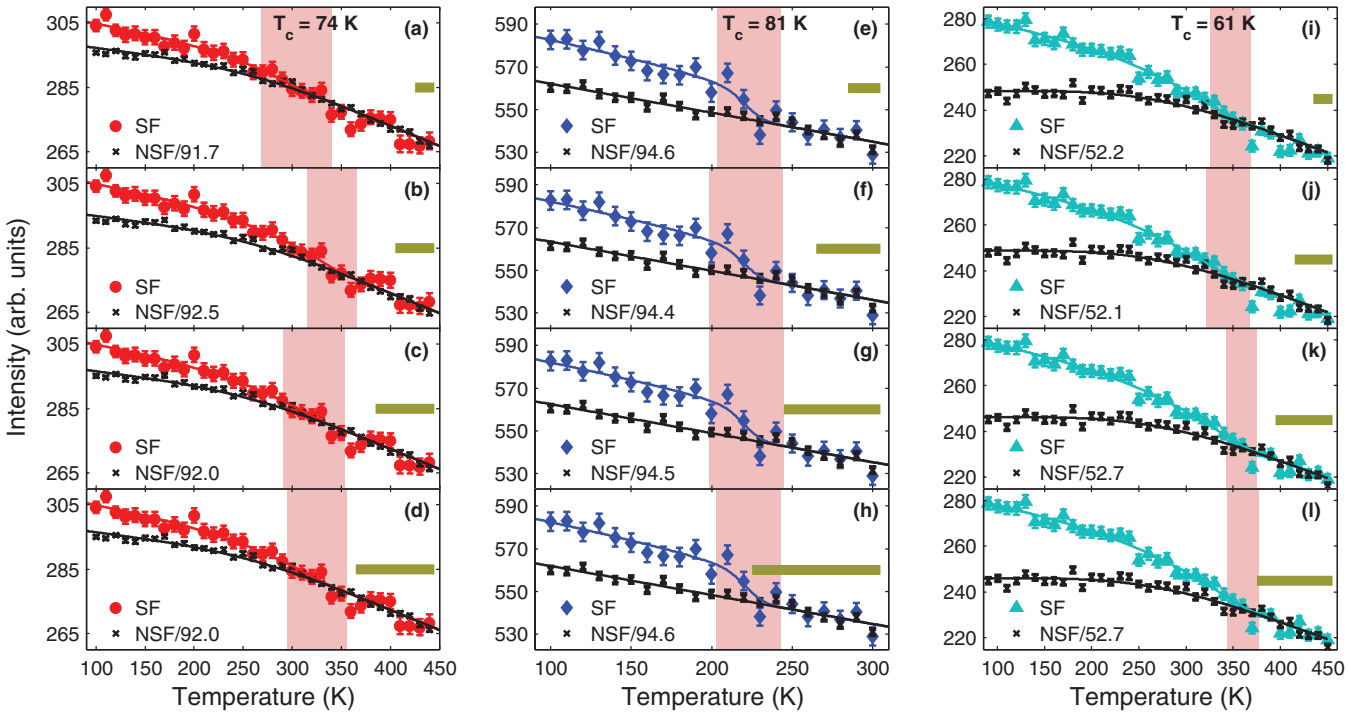

FIG. 2. (Color online) Demonstration of the insensitivity of the extracted T_{mag} to the temperature range over which the NSF intensity is rescaled to match the SF intensity. T_{mag} is estimated by fitting the deviation of the SF data from the (rescaled) NSF data to a power law. The fit values and errors (one standard deviation) are indicated by the position and width of the vertical bands. The temperature ranges of the normalization are indicated by the horizontal bars. (a–d): $\mathbf{P} \parallel \mathbf{Q}$ data for the $T_c = 74$ K underdoped sample studied in this work. (e–l): previous data for a sample that was studied at two distinct oxygen (and hence hole) concentrations.[5]

in the high-temperature range, where no magnetic signal is expected and all intensity in the SF geometry is assumed to be due to leakage of nuclear scattering. Upon cooling, the NSF intensity gradually increases in a fashion consistent with the Debye-Waller factor, whereas the SF intensity increases more rapidly and deviates from the (rescaled) NSF data below $T_{mag} \approx 320$ K. This deviation marks the onset of a magnetic signal, and is more clearly seen when data from all three polarization geometries are averaged to reduce the statistical error [Fig. 1(d)]. After subtracting the (rescaled) NSF data as background, the increase of the SF signal below T_{mag} is continuous, consistent with a second-order phase transition [Fig. 1(e)]. These data are highly consistent with the previous results.[5] In particular, $T_{mag} \approx 320$ K and the ordered moment ($\sim$0.5 mbarn at 100 K) lie between the values established for lower and higher doping levels. The conversion of signal intensity to absolute units is achieved through a comparison with the intensity of the (1 0 1) nuclear Bragg reflection, which is calculated to be 1.26 barn based on the composition and crystal structure of Hg1201, given that the observed extra spin-flip intensity at 100 K in Fig. 1 is about 0.038% of the non-spin-flip intensity after considering the flipping ratio of ≈ 90. The vertical band in 1(d) and 1(e) indicates the uncertainty in T_{mag}.

The analysis in Fig. 1 (and in Refs. 3–5 and 9) relies on the assumption that there exists no magnetic signal at the highest measurement temperature. This introduces a potential error in the determination of T_{mag}: if one were to extend the measurement to even higher temperature, one might observe a higher T_{mag}. In Fig. 2, we show that this is very unlikely by performing a stability test for the analysis of the $\mathbf{P} \parallel \mathbf{Q}$ data in Fig. 1(a), as well as for the prior results for Hg1201.[5] By rescaling the NSF data to match the SF data over different temperature ranges, we find that the extracted value of T_{mag} is robust and exhibits no systematic dependence on the choice of the temperature range.

An alternative, assumption-free analysis is presented in Fig. 3, which further demonstrates that the observed onset of the magnetic signal is independent of the treatment of the NSF data. We define the *average flipping ratio*

$$R_{avg}(T) \equiv \frac{\sum_{T'>T} I_{NSF}(T')}{\sum_{T'>T} I_{SF}(T')}, \qquad (1)$$

where $I_{SF}(T')$ and $I_{NSF}(T')$ are the SF and NSF intensities measured at temperature T', respectively. Since $R_{avg}(T)$ is defined over a temperature range above T and up to the highest measured temperature, it is determined with better and better statistical precision as T decreases [compared to the flipping ratio $R(T)$ defined at individual temperatures], and a downward kink-like behavior is expected at the onset temperature of any magnetic signal (if the transition is reasonably sharp). Importantly, in the presence of a weak extrinsic effect (such as sample misalignment or movement relative to the neutron beam) which might cause a drift in $R(T)$ versus temperature, $R_{avg}(T)$ is expected to remain featureless apart from having a finite slope (i.e., without a "kink").

Figure 3 displays the average-flipping-ratio analysis of the data in Fig. 1 and of those reported in Ref. 5. Indeed, a kink

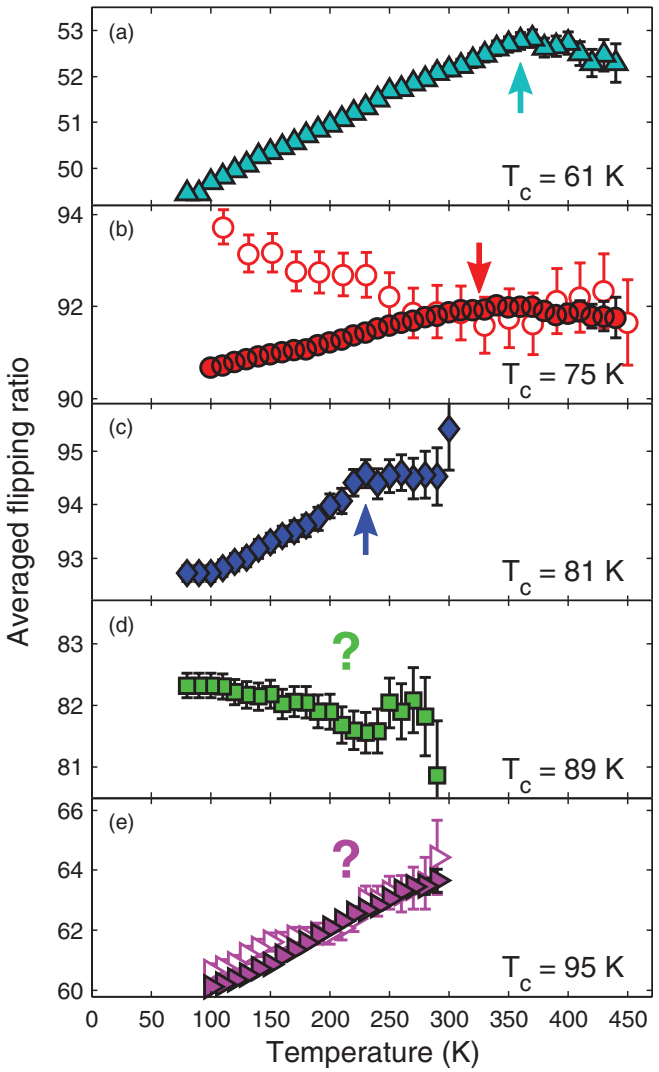

FIG. 3. (Color online) Average flipping ratio (see text) measured on five different samples. The onset temperatures of the magnetic signal are indicated by arrows for the three most underdoped samples, where they can be reliably determined with this unbiased method. Filled symbols: (1 0 1) data. Empty symbols: (0 0 3) reference data. The (0 0 3) results are rescaled (vertically) for better comparison.

followed by faster decrease of $R_{avg}(T)$ toward low temperature is observed at about the same T_{mag} as reported in Ref. 5 and in Fig. 1 for the three most underdoped samples. The extracted T_{mag} values decrease monotonically with increasing doping. No clear effect is observed for the $T_c = 89$ K and 95 K samples.

For the $T_c = 75$ K sample, we measured the (0 0 3) reflection for calibration purposes (see below). The average-flipping-ratio analysis does not show an effect at this reflection, in stark contrast with the observation at the (1 0 1) reflection [Fig. 3(b)]. The absence of a spin-flip magnetic signal at (0 0 3) could have two reasons: (1) the magnetic moments in each Cu-O plane cancel each other, which would lead to a vanishing magnetic structure factor for $H = K = 0$; (2) the magnetic moments are parallel to the c axis and are hence not detectable with $\mathbf{Q} \parallel \mathbf{c}$. This observation is consistent with "intra-unit-cell antiferromagnetic order" that arises from either spin moments[3,10] or orbital currents[24,31,32] within the CuO_2 layers.

With this in mind, however, a closer look at the data in Fig. 3(e) for the $T_c = 95$ K sample suggests that there might even be a small effect at the (1 0 1) reflection below $T_{mag} \sim 200$ K, as the data deviate from the (0 0 3) reference. This difference is rather marginal and needs to be confirmed through further measurements. Nevertheless, we note that $T_{mag} \sim 200$ K would be consistent with the value of T^* determined from resistivity measurements and with the temperature below which inelastic neutron scattering reveals the presence of magnetic excitations at the same doping.[36] Similarly, a small elastic magnetic signal may be present in the $T_c = 89$ K sample, for which the (0 0 3) reflection was not measured. We therefore caution that it is premature to conclude whether there is a $q = 0$ magnetic diffraction signal near optimal doping: While the signal would have to be weak and/or the order may have become short-range, the related pseudogap magnetic excitations revealed in our recent inelastic neutron scattering study are still clearly present at optimal doping.[36]

The fact that $R_{avg}(T)$ may exhibit a nonzero temperature dependence without showing a "kink" [e.g., the (0 0 3) reflection in Figs. 3(b) and 3(e)] indicates an experimental issue unrelated to the $q = 0$ magnetic signal. The exact cause for this is unknown, but most likely this extrinsic effect is related to tiny sample movements during temperature changes. Such movements would change the scattering beam path and hence the degree of the spin polarization, leading to a temperature-dependent flipping ratio. The effect was largest for the $T_c = 95$ K sample which was co-mounted on a delicate sample holder [Fig. 3(e)]. It was not noticed in early measurements of YBCO and Hg1201 (Refs. 3 and 5), but it was found and corrected for in the more recent studies of YBCO,[4,9] through measurements of a reference Bragg reflection. The primary undesirable consequence of this extrinsic effect is a systematic error in the estimate of the magnitude of the magnetic signal based on the type of analysis in Fig. 1. In order to correct for this error for the $T_c = 75$ K sample, we measured $R(T)$ at the (0 0 3) reflection in all three polarization geometries, and approximated the results by linear functions of T (Fig. 4, left panels). The (0 0 3) reflection was chosen as the reference because its scattering angle (2θ) differs from that of the (1 0 1) reflection by only 4.5°, which ensures that the scattering beam paths and the guide-field profiles are very similar. The linear fits to $R(T)$ for the (0 0 3) reflection are then rescaled to the high-temperature values of $R(T)$ measured at the (1 0 1) reflection, which we treat as an estimate of the underlying $R_0(T)$ of the (1 0 1) reflection in the absence of a magnetic signal. This analysis is illustrated in the right panels of Fig. 4, where the underlying $R_0(T)$ and the confidence range of our estimate are indicated by solid and dashed lines, respectively.

Using the estimated $R_0(T)$ and the NSF intensity measured at the (1 0 1) reflection, the nuclear Bragg intensity leakage in the SF geometry can be calculated. The difference between the measured total SF intensity and the estimated nuclear intensity leakage is the genuine magnetic signal. Figure 5 displays the (1 0 1) magnetic intensities I_{mag} for all three spin-polarization geometries. The results have been converted into absolute units of scattering crosssection based on the calculated crosssection

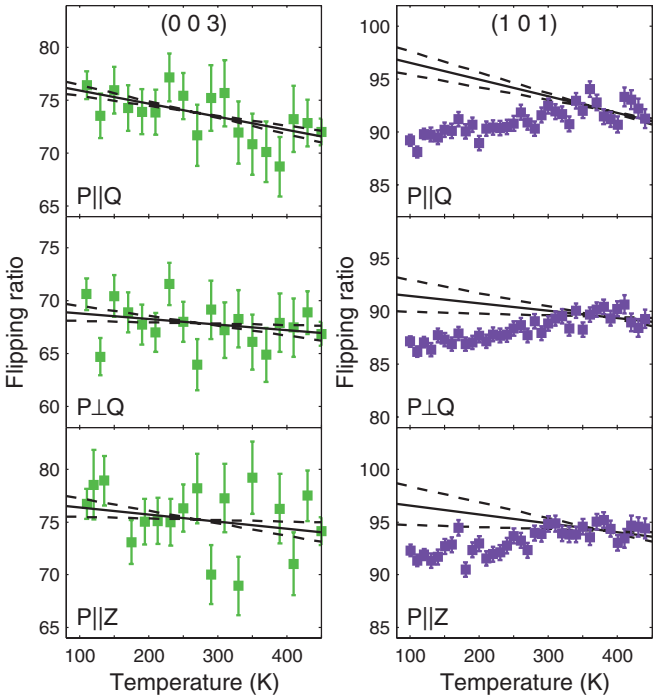

FIG. 4. (Color online) (Left panels) Flipping ratio $R(T)$ at the (0 0 3) reflection for the $T_c = 75$ K sample. Solid lines are linear fits to the data, and dashed lines represent the confidence range of the estimated linear slopes (one sigma). (Right panels) $R(T)$ for the (1 0 1) reflection. Solid and dashed lines are obtained by rescaling the corresponding linear fits in the left panels to match the data above $T = 330$ K, which serves as an estimate of the underlying $R_0(T)$ in the absence of a magnetic signal.

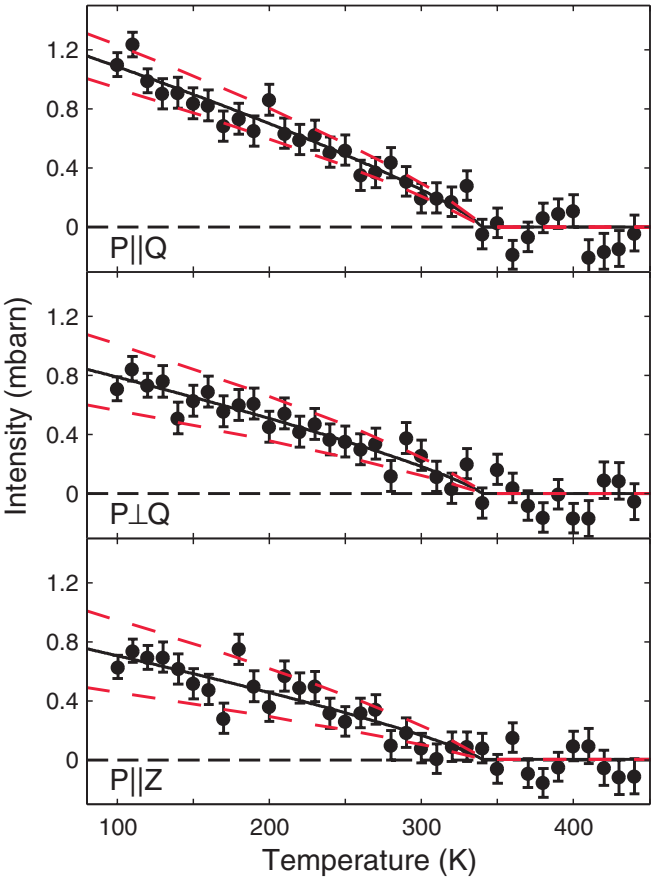

FIG. 5. (Color online) Magnetic intensities at the (1 0 1) reflection for the $T_c = 75$ K sample, obtained by subtracting from the SF intensities the NSF intensities divided by temperature-dependent $R_0(T)$ determined from Fig. 4. Dashed lines indicate uncertainty (one standard deviation) due to the slope estimates in Fig. 4.

of the (1 0 1) nuclear reflection, as discussed above. The magnitude of the magnetic signal contains two primary sources of error (indicated by the dashed lines in Fig. 5): the statistical error in the measured (1 0 1) SF intensity and the uncertainty in determining the slope of $R_0(T)$ at the (0 0 3) reflection.

A comparison of the extracted magnetic signal in Figs. 1 and 5 shows that the systematic error brought about by the extrinsic effect on $R_0(T)$ can be rather substantial. As a self-consistency check, we find that the magnetic signal in the $\mathbf{P} \parallel \mathbf{Q}$ geometry equals, within error, the sum of the intensities in the $\mathbf{P} \perp \mathbf{Q}$ and $\mathbf{P} \parallel \mathbf{Z}$ geometries. This is an expected result, since the spin-flip scattering probability is proportional to the square of the magnetic moments perpendicular to both $\mathbf{Q}$ and $\mathbf{P}$. We find that this sum rule is better satisfied after the calibration based on $R(T)$ measured at the (0 0 3) reflection, which confirms that this calibration is indeed meaningful. An important observation from Fig. 5 is that the intensities in the $\mathbf{P} \perp \mathbf{Q}$ and $\mathbf{P} \parallel \mathbf{Z}$ geometries are approximately the same. Since the direction of $\mathbf{Q} = (1\,0\,1)$ is rather close to $\mathbf{a}^*$, and because the horizontal scattering plane is perpendicular to $\mathbf{b}^*$, $I_{\mathrm{mag},P\parallel Z}$ primarily measures the magnetic moments along the c axis. On the other hand, $I_{\mathrm{mag},P\perp Q}$ measures the magnetic moments along the b axis (the same magnetic component has to exist along the a axis, since a and b are equivalent in the tetragonal structure of Hg1201). Therefore the fact that $I_{\mathrm{mag},P\perp Q} \approx I_{\mathrm{mag},P\parallel Z}$ suggests that the magnetic moments are pointing in a direction that is neither parallel nor perpendicular to the CuO_2 layers, but instead lie $45 \pm 25^\circ$ away from the c axis. This is consistent with the previous results for YBCO,[3,4] Hg1201,[5] and LSCO.[8]

For the $T_c = 75$ K sample, the values of I_{mag} extracted before and after the (0 0 3) calibration differ by 0.4–0.6 mbarn. The need for such a calibration for this sample implies that, in the previous results reported in Ref. 5, the error in the signal amplitudes was likely underestimated, as only statistical errors were considered. This might also explain why no signal was identified for the $T_c = 89$ K sample, while a signal may even be present in the $T_c = 95$ K sample, as discussed above (Fig. 3). On the other hand, the error due to the extrinsic effect on $R(T)$ cannot be overwhelmingly large, as otherwise one would not be able to extract magnetic signals as small as 0.5 mbarn or to arrive at very similar signal amplitudes for two samples at almost the same doping.[5] We emphasize that the extracted T_{mag} values for the $T_c = 75$ K sample do not differ substantially before and after the calibration (by less than 20 K), and thus the rather good agreement between T_{mag} and T^* extracted from planar resistivity measurements remains intact. Taking all the factors into account, for the previous results for Hg1201 reported in Ref. 5, we arrive at the new error estimate of ~ 0.3 mbarn on I_{mag} for the $T_c = 79$ K and 81 K samples, and

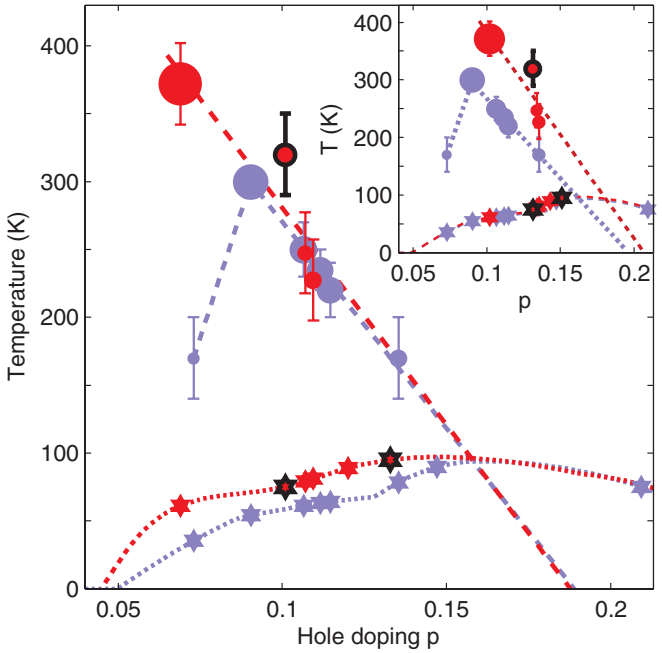

FIG. 6. (Color online) Phase diagram of Hg1201 (red) and YBCO (light blue) at intermediate doping. Stars and circles represent T_c and T_{mag}, respectively. Data for the two new Hg1201 samples studied in the present work are indicated by black borders. Data for YBCO are from the literature (Refs. 3,4 and 9). Symbols for T_{mag} are plotted with their area proportional to the magnetic intensities. In the main panel, hole doping for Hg1201 is determined from the $T_c(p)$ relationship according to Ref. 37. In the inset, the hole concentration of Hg1201 is estimated based on the same $T_c(p)$ relationship as in YBCO (Ref. 38) (after rescaling the maximal T_c to 97 K).

of ~ 0.5 mbarn for the most underdoped, $T_c = 61$ K sample. We conservatively estimate an error of 30 K in the extracted values of T_{mag} for Hg1201. Figure 6 shows the updated phase diagram, which also includes the prior work for YBCO.

IV. DISCUSSION

Before discussing the physical meaning of the $q = 0$ order, we first comment on the robustness of its observation using spin-polarized neutron diffraction. Our data in Figs. 1–5 demonstrate that the observation of a magnetic signal below T_{mag} is independent of the data analysis method. It is furthermore consistent with the decrease of T^* toward higher hole concentration and the disappearance of the pseudogap phenomenon near optimal doping. Moreover, as already shown in our prior work[5] and discussed further below, our data for single-layer Hg1201 are in good agreement with those for double-layer YBCO.[3,4,9] These results clearly imply that, at least in compounds with high maximal values of T_c, the pseudogap phenomenon is a phase transition rather than a mere crossover.

In Ref. 4, an attempt was made to determine the critical exponent of the transition. While the reported value of $2\beta = 0.37 \pm 0.12$ is consistent with our data, we caution that the fit value depends on the correction for the extrinsic temperature dependence of the flipping ratio (Fig. 5). The uncertainty in the latter procedure should be considered in comparisons with theoretical predictions.

Recent local-probe μSR (Refs. 39 and 40) and NMR/NQR (Refs. 41 and 42) experiments indicate only very weak internal magnetic fields in several underdoped cuprates. We note that these findings are not necessarily inconsistent with our observations. First, as can be seen from our neutron scattering results for samples with $T_c > 81$ K (Fig. 3), the magnetic Bragg signal becomes weak or even disappears close to optimal doping, consistent with results for YBCO. Therefore, local-probe measurement of compounds close to optimal doping may fail to see the order. Second, whereas in the antiferromagnetic cuprate parent compounds the internal magnetic field deduced from μSR generally agrees with the size of local spin moments observed by neutron diffraction, the internal field deduced from NQR is smaller by a factor of three.[43] This considerable uncertainty in the quantitative estimation of internal fields does not appear to have been taken into account in the upper bound estimate in Ref. 42.

Third, depending on details of the magnetic structure observed in neutron diffraction, the magnetic field at atomic sites probed by NMR/NQR can be expected to vary significantly. For instance, the model with spins at the oxygen sites discussed in Refs. 3 and 10 does not produce any field at the Ba site of the compound $YBa_2Cu_4O_8$ studied in Ref. 42 if the moments point along c^*. It has been proposed that the magnetic order observed in our experiments results from circulating charge currents rather than local moments.[24,32] Point-dipole calculations as performed in Ref. 42 might then yield rather inaccurate estimates of the true magnetic field at the Ba site. Fourth, if the magnetic order observed in our experiments indeed results from circulating charge currents,[24,32] the implanted muons in μSR experiments might perturb this state sufficiently strongly to render this probe unsuitable for its detection.[44,45]

Finally, the time scales of the local probes are many orders of magnitude slower than that of our neutron scattering experiment. A rapidly fluctuating field on the former time scales would therefore substantially reduce the effective internal field observed by the local probes, but would appear static when measured with neutrons. A well-known example is the "stripe" order in the La-based cuprates: While the order is clearly seen with x rays and neutrons,[26] NMR evidence[46] is relatively weak or indirect, and the ordering temperatures deduced from the onset of the internal fields seen by NMR[46] and μSR[47] are considerably lower than those observed by scattering methods. Similar "glassy" behavior is found in very underdoped YBCO, for which the spin-density-wave ordering temperature is strongly dependent on the probe frequency.[29,48]

In Fig. 6, we estimate the hole concentrations p in Hg1201 and YBCO based on values of T_c. The estimate for YBCO is the same in both the main panel and the inset, following the empirical relationship reported in Ref. 38. For Hg1201, the estimate in the main panel is based on the reported relationship between T_c and the Seebeck coefficient at room temperature,[37] and in the inset it is assumed that $T_c(p)$ is the same as that for YBCO, apart from a scale factor for the maximal T_c (94 K for

YBCO and 97 K for Hg1201). The two scenarios lead to the following considerations: (i) In the main panel, $T_{mag}(p)$ for Hg1201 ($0.07 < p < 0.11$) and YBCO ($0.09 < p < 0.135$) in the respective ranges of p can be well approximated by the same linear function of p, which extrapolates to $T_{mag} = 0$ K around $p_c = 0.19$. This is precisely where a quantum critical point has been previously proposed.[49] (ii) In the inset, even though the estimated hole concentrations for Hg1201 are different from those in the main panel, a linear fit to the data nevertheless extrapolates to $T_{mag} = 0$ at $p_c \approx 0.20$, consistent (within error) with p_c for YBCO. (iii) It was recently found that T_{mag} for heavily underdoped $YBCO_{6.45}$ is substantially smaller than for $YBCO_{6.5}$, and that the size of the ordered moment is dramatically reduced.[9] This may be an indication that the $q = 0$ magnetic order and the SDW order found in heavily underdoped YBCO[28,29] compete with each other. A similar scenario may explain why the $q = 0$ order in LSCO is short range and only develops at relatively low temperature.[8,10] The balance of the competition may furthermore be modified by disorder, such as Zn impurities,[9] which suggests that the stability of each phase also depends on material-specific parameters. In Hg1201, if the $T_c(p)$ relationship in the main panel is correct, it would necessarily imply that a competition between the SDW and the $q = 0$ order is either absent in Hg1201 or only occurs at much lower doping than in YBCO. However, if the $T_c(p)$ relationship in the inset is correct, then the $q = 0$ order in Hg1201 has not yet been investigated to a hole concentration as low as in $YBCO_{6.45}$, and no conclusion can be drawn at this point regarding its competition with the SDW order, which so far has not been identified in Hg1201. Future measurements of Hg1201 at lower doping are clearly desirable to address this open question. (iv) The $T_c(p)$ relationship in the inset implies that the $q = 0$ magnetic signal disappears above $p \sim 0.14$ in both Hg1201 and YBCO. However, we caution that this may be related to an insufficient sensitivity of our technique to small magnetic signals, and that long-range magnetic order may well exist in Hg1201 up to optimal doping [Fig. 3(e)], as discussed in Sec. III. Recent inelastic neutron scattering experiments revealed prominent magnetic excitations that are likely associated with the $q = 0$ order.[36] The inelastic signal near optimal doping was observed (in the same $T_c = 95$ K sample) below ~ 200 K, consistent with the extrapolated value of T_{mag} at this doping, no matter whether the doping scenario in the main panel or in the inset is considered.

In principle, the real-space magnetic ordering pattern should be obtainable from an extensive study of the magnetic Bragg intensity as a function of momentum transfer $\mathbf{Q}$ and neutron spin polarization $\mathbf{P}$. Unfortunately, this has remained a formidable challenge for several reasons. First, the magnetic signal coincides with nuclear Bragg reflections, so that the former is discernible only when the latter are relatively weak, and presumably only at relatively low $|\mathbf{Q}|$, where the magnetic signal is sufficiently strong. This restricts our measurements to only a few Bragg reflections. Second, full polarization analysis requires very high and stable flipping ratios in all three polarization geometries. This is usually not simultaneously attainable for all reflections: While it is required that the profile of the guide field exhibits no abrupt change along the neutron beam path, which can differ substantially among the reflections, the placement of the Helmholtz coils can only be optimized for some, but not all beam paths. Third, the extrinsic temperature dependence of $R(T)$ is difficult to remove through calibration measurements at the level of accuracy that is needed for a detailed polarization analysis, and a nearby, nonmagnetic reference Bragg reflection is not always available. Notably, these difficulties all stem from the fact that the magnetic reflections coincide with the much stronger nuclear Bragg peaks. Nevertheless, there are promising alternative routes to obtain further information. For example, it should be possible to measure the in-plane magnetic form factor away from nuclear Bragg peaks if the $q = 0$ order is short-range and two-dimensional, such as in LSCO.[8] Furthermore, quantitative information from the measurement of the associated excitations[36] can be expected to help elucidate the nature of the underlying magnetism.

Finally, we note that while at first sight the comparable magnetic intensities in the $\mathbf{P} \perp \mathbf{Q}$ and $\mathbf{P} \parallel \mathbf{Z}$ geometries (Fig. 5) would seem to require either tilted spin moments or orbital currents that flow out of the CuO_2 layers (e.g., involving the apical oxygen[50]), this semiclassical picture may not be correct. It has been recently pointed out that effective tilted moments may arise from purely in-plane orbital currents once the quantum superposition of the classical loop patterns is taken into account.[51] The main constraints our neutron diffraction results place on theoretical ideas are the fact that the magnetic order appears below the pseudogap temperature and that it requires an even number of moments per primitive cell even in Hg1201, the cuprate with arguably the simplest crystal structure. With the current experimental capabilities, the extent to which we can directly determine the exact location of the moments and how they are generated is unfortunately rather limited.

V. CONCLUSION

We have carried out a systematic polarized-neutron diffraction study of the $q = 0$ magnetic order in the pseudogap phase of Hg1201. The results presented here for an underdoped and an optimally doped sample are consistent with our prior work. A comparison with YBCO leads to two distinctly different scenarios for the underdoped side of the phase diagram, and future measurements of Hg1201 at even lower doping are required to select among the two possibilities. While technical difficulties prevent us from determining the real-space ordering pattern, such difficulties may be partially circumvented in future studies of the short-range versions of the order and of the associated fundamental magnetic excitations.

ACKNOWLEDGMENTS

We wish to thank M.-H. Julien, A. Kapitulnik, and C. M. Varma for valuable comments. This work was supported by the DOE under Contract No. DEAC02-76SF00515 and by the NSF under Grant No. DMR-0705086. Y.L. acknowledges support from the Alexander von Humboldt foundation.

*Present address: Max Planck Institute for Solid State Research, D-70569 Stuttgart, Germany.
†greven@physics.umn.edu

[1] M. R. Norman, D. Pines, and C. Kallin, Adv. Phys. **54**, 715 (2005).
[2] A. Kaminski, S. Rosenkranz, H. M. Fretwell, J. C. Campuzano, Z. Li, H. Raffy, W. G. Cullen, H. You, C. G. Oison, C. M. Varma, and H. Höchst, Nature (London) **416**, 610 (2002).
[3] B. Fauqué, Y. Sidis, V. Hinkov, S. Pailhès, C. T. Lin, X. Chaud, and P. Bourges, Phys. Rev. Lett. **96**, 197001 (2006).
[4] H. A. Mook, Y. Sidis, B. Fauqué, V. Balédent, and P. Bourges, Phys. Rev. B **78**, 020506 (2008).
[5] Y. Li, V. Balédent, N. Barišić, Y. Cho, B. Fauqué, Y. Sidis, G. Yu, X. Zhao, P. Bourges, and M. Greven, Nature (London) **455**, 372 (2008).
[6] J. Xia, E. Schemm, G. Deutscher, S. A. Kivelson, D. A. Bonn, W. N. Hardy, R. Liang, W. Siemons, G. Koster, M. M. Fejer, and A. Kapitulnik, Phys. Rev. Lett. **100**, 127002 (2008).
[7] B. Leridon, P. Monod, D. Colson, and A. Forget, Europhys. Lett. **87**, 17011 (2009).
[8] V. Balédent, B. Fauqué, Y. Sidis, N. B. Christensen, S. Pailhès, K. Conder, E. Pomjakushina, J. Mesot, and P. Bourges, Phys. Rev. Lett. **105**, 027004 (2010).
[9] V. Balédent, D. Haug, Y. Sidis, V. Hinkov, C. T. Lin, and P. Bourges, Phys. Rev. B **83**, 104504 (2011).
[10] P. Bourges and Y. Sidis, C. R. Physique **12**, 461 (2011).
[11] R. Daou, J. Chang, D. LeBoeuf, O. Cyr-Choinière, F. Laliberté, N. Doiron-Leyraud, B. J. Ramshaw, R. Liang, D. A. Bonn, W. N. Hardy, and L. Taillefer, Nature (London) **463**, 519 (2010).
[12] M. Hashimoto, R.-H. He, K. Tanaka, J. P. Testaud, W. Meevasana, R. G. Moore, D. H. Lu, H. Yao, Y. Yoshida, H. Eisaki, T. P. Devereaux, Z. Hussain, and Z.-X. Shen, Nat. Phys. **6**, 414 (2010).
[13] R.-H. He, M. Hashimoto, H. Karapetyan, J. D. Koralek, J. P. Hinton, J. P. Testaud, V. Nathan, Y. Yoshida, H. Yao, K. Tanaka, W. Meevasana, R. G. Moore, D. H. Lu, S.-K. Mo, M. Ishikado, H. Eisaki, Z. Hussain, T. P. Devereaux, S. A. Kivelson, J. Orenstein, A. Kapitulnik, and Z.-X. Shen, Science **331**, 1579 (2011).
[14] M. J. Lawler, K. Fujita, J. Lee, A. R. Schmidt, Y. Kohsaka, C. K. Kim, H. Eisaki, S. Uchida, J. C. Davis, J. P. Sethna, and E.-A. Kim, Nature (London) **466**, 347 (2010).
[15] S. Doniach and M. Inui, Phys. Rev. B **41**, 6668 (1990).
[16] V. J. Emery and S. A. Kivelson, Nature (London) **374**, 434 (1995).
[17] J. Corson, R. Mallozzi, J. Orenstein, J. N. Eckstein, and I. Bozovic, Nature (London) **398**, 221 (1999).
[18] N. Bergeal, J. Lesueur, M. Aprili, G. Faini, J. P. Contour, and B. Leridon, Nat. Phys. **4**, 608 (2008).
[19] J. Lee, K. Fujita, A. R. Schmidt, C. K. Kim, H. Eisaki, S. Uchida, and J. C. Davis, Science **325**, 1099 (2009).
[20] M. S. Grbić, N. Barišić, A. Dulčić, I. Kupčić, Y. Li, X. Zhao, G. Yu, M. Dressel, M. Greven, and M. Požek, Phys. Rev. B **80**, 094511 (2009).
[21] H.-H. Wen, G. Mu, H. Luo, H. Yang, L. Shan, C. Ren, P. Cheng, J. Yan, and L. Fang, Phys. Rev. Lett. **103**, 067002 (2009).
[22] M. S. Grbić, M. Požek, D. Paar, V. Hinkov, M. Raichle, D. Haug, B. Keimer, N. Barišić, and A. Dulčić, Phys. Rev. B **83**, 144508 (2011).
[23] L. S. Bilbro, R. Valdés Aguilar, G. Logvenov, O. Pelleg, I. Božović, and N. P. Armitage, Nat. Phys. **7**, 298 (2011).
[24] C. M. Varma, Phys. Rev. B **55**, 14554 (1997).
[25] A. R. Moodenbaugh, Y. Xu, M. Suenaga, T. J. Folkerts, and R. N. Shelton, Phys. Rev. B **38**, 4596 (1988).
[26] J. M. Tranquada, B. J. Sternlieb, J. D. Axe, Y. Nakamura, and S. Uchida, Nature (London) **375**, 561 (1995).
[27] K. Yamada, C. H. Lee, K. Kurahashi, J. Wada, S. Wakimoto, S. Ueki, H. Kimura, Y. Endoh, S. Hosoya, G. Shirane, R. J. Birgeneau, M. Greven, M. A. Kastner, and Y. J. Kim, Phys. Rev. B **57**, 6165 (1998).
[28] V. Hinkov, D. Haug, B. Fauque, P. Bourges, Y. Sidis, A. Ivanov, C. Bernhard, C. T. Lin, and B. Keimer, Science **319**, 597 (2008).
[29] D. Haug, V. Hinkov, Y. Sidis, P. Bourges, N. B. Christensen, A. Ivanov, T. Keller, C. T. Lin, and B. Keimer, New J. Phys. **12**, 105006 (2010).
[30] H. Eisaki, N. Kaneko, D. L. Feng, A. Damascelli, P. K. Mang, K. M. Shen, Z.-X. Shen, and M. Greven, Phys. Rev. B **69**, 064512 (2004).
[31] M. E. Simon and C. M. Varma, Phys. Rev. Lett. **89**, 247003 (2002).
[32] C. M. Varma, Phys. Rev. B **73**, 155113 (2006).
[33] X. Zhao, G. Yu, Y.-C. Cho, G. Chabot-Couture, N. Barišić, P. Bourges, N. Kaneko, Y. Li, L. Lu, E. M. Motoyama, O. P. Vajk, and M. Greven, Adv. Mater. **18**, 3243 (2006).
[34] N. Barišić, Y. Li, X. Zhao, Y.-C. Cho, G. Chabot-Couture, G. Yu, and M. Greven, Phys. Rev. B **78**, 054518 (2008).
[35] Y. Li, N. Egetenmeyer, J. L. Gavilano, N. Barišić, and M. Greven, Phys. Rev. B **83**, 054507 (2011).
[36] Y. Li, V. Balédent, G. Yu, N. Barišić, K. Hradil, R. A. Mole, Y. Sidis, P. Steffens, X. Zhao, P. Bourges, and M. Greven, Nature (London) **468**, 283 (2010).
[37] A. Yamamoto, W.-Z. Hu, and S. Tajima, Phys. Rev. B **63**, 024504 (2000).
[38] R. Liang, D. A. Bonn, and W. N. Hardy, Phys. Rev. B **73**, 180505 (2006).
[39] G. J. MacDougall, A. A. Aczel, J. P. Carlo, T. Ito, J. Rodriguez, P. L. Russo, Y. J. Uemura, S. Wakimoto, and G. M. Luke, Phys. Rev. Lett. **101**, 017001 (2008).
[40] J. E. Sonier, V. Pacradouni, S. A. Sabok-Sayr, W. N. Hardy, D. A. Bonn, R. Liang, and H. A. Mook, Phys. Rev. Lett. **103**, 167002 (2009).
[41] S. Strässle, J. Roos, M. Mali, H. Keller, and T. Ohno, Phys. Rev. Lett. **101**, 237001 (2008).
[42] S. Strässle, B. Graneli, M. Mali, J. Roos, and H. Keller, Phys. Rev. Lett. **106**, 097003 (2011).
[43] A. Lombardi, M. Mali, J. Roos, and D. Brinkmann, Phys. Rev. B **53**, 14268 (1996).
[44] A. Shekhter, L. Shu, V. Aji, D. E. MacLaughlin, and C. M. Varma, Phys. Rev. Lett. **101**, 227004 (2008).
[45] H. T. Dang, E. Gull, and A. J. Millis, Phys. Rev. B **81**, 235124 (2010).
[46] A. W. Hunt, P. M. Singer, A. F. Cederström, and T. Imai, Phys. Rev. B **64**, 134525 (2001).
[47] B. Nachumi, Y. Fudamoto, A. Keren, K. M. Kojima, M. Larkin, G. M. Luke, J. Merrin, O. Tchernyshyov, Y. J. Uemura, N. Ichikawa, M. Goto, H. Takagi, S. Uchida, M. K. Crawford, E. M. McCarron, D. E. MacLaughlin, and R. H. Heffner, Phys. Rev. B **58**, 8760 (1998).
[48] F. Coneri, S. Sanna, K. Zheng, J. Lord, and R. De Renzi, Phys. Rev. B **81**, 104507 (2010).
[49] J. L. Tallon and J. W. Loram, Physica C **349**, 53 (2001).
[50] C. Weber, A. Läuchli, F. Mila, and T. Giamarchi, Phys. Rev. Lett. **102**, 017005 (2009).
[51] Y. He and C. M. Varma, Phys. Rev. Lett. **106**, 147001 (2011).